

# Puzzling Variation of Gamma Rays from the Sun over the Solar Cycle Revealed with *Fermi*-LAT

A. ACHARYYA,<sup>1</sup> A. ADELIO,<sup>2</sup> M. AJELLO,<sup>3</sup> L. BALDINI,<sup>4,5</sup> C. BARTOLINI,<sup>6,7</sup> D. BASTIERI,<sup>8,9,10</sup> J. BECERRA GONZALEZ,<sup>11</sup>  
R. BELLAZZINI,<sup>5</sup> B. BERENJI,<sup>12</sup> E. BISSALDI,<sup>13,6</sup> R. D. BLANDFORD,<sup>14</sup> R. BONINO,<sup>15,16</sup> E. BOTTACINI,<sup>9,14</sup> S. BUSON,<sup>17,18</sup>  
R. A. CAMERON,<sup>14</sup> P. A. CARAVEO,<sup>19</sup> F. CASABURO,<sup>20,21,22</sup> F. CASINI,<sup>23</sup> E. CAVAZZUTI,<sup>24</sup> D. CERASOLE,<sup>13,6</sup> S. CIPRINI,<sup>20,21</sup>  
G. COZZOLONGO,<sup>25,26</sup> P. CRISTARELLA ORESTANO,<sup>23,2</sup> A. CUOCO,<sup>15,16</sup> S. CUTINI,<sup>2</sup> F. D'AMMANDO,<sup>27</sup> D. DEPALO,<sup>6,13</sup>  
S. W. DIGEL,<sup>14</sup> N. DI LALLA,<sup>14</sup> L. DI VENERE,<sup>6</sup> A. DOMÍNGUEZ,<sup>28</sup> A. FIORI,<sup>29</sup> Y. FUKAZAWA,<sup>30</sup> P. FUSCO,<sup>13,6</sup>  
F. GARGANO,<sup>6</sup> C. GASBARRA,<sup>20,31</sup> D. GASPARRINI,<sup>20,21</sup> S. GERMANI,<sup>32,2</sup> F. GIACCHINO,<sup>20,21</sup> N. GIGLIETTO,<sup>13,6</sup>  
F. GIORDANO,<sup>13,6</sup> M. GIROLETTI,<sup>27</sup> S. GUIREC,<sup>33,34</sup> R. GUPTA,<sup>34</sup> M. HASHIZUME,<sup>30</sup> E. HAYS,<sup>34</sup> J.W. HEWITT,<sup>35</sup>  
A. HOLZMANN AIRASCA,<sup>7,6</sup> D. HORAN,<sup>36</sup> X. HOU,<sup>37</sup> T. KAYANOKI,<sup>30</sup> M. KUSS,<sup>5</sup> S. LARSSON,<sup>38,39</sup> A. LAVIRON,<sup>34,40</sup>  
J. LI,<sup>41,42</sup> I. LIODAKIS,<sup>43</sup> F. LONGO,<sup>44,45</sup> F. LOPARCO,<sup>13,6</sup> S. LÓPEZ PÉREZ,<sup>36</sup> M. N. LOVELLETTE,<sup>46</sup> P. LUBRANO,<sup>2</sup>  
S. MALDERA,<sup>15</sup> A. MANFREDI,<sup>5</sup> G. MARTÍ-DEVEZA,<sup>44</sup> R. MARTINELLI,<sup>44,45</sup> M. N. MAZZIOTTA,<sup>6</sup> J. E. MCENERY,<sup>34,47</sup>  
I. MEREU,<sup>2,23</sup> M. MICHAELIDIS,<sup>14</sup> P. F. MICHELSON,<sup>14</sup> N. MIRABAL,<sup>34,48</sup> T. MIZUNO,<sup>49</sup> P. MONTI-GUARNIERI,<sup>44,45</sup>  
M. E. MONZANI,<sup>14,50</sup> A. MORSELLI,<sup>20</sup> I. V. MOSKALENKO,<sup>14</sup> M. NEGRO,<sup>51</sup> N. OMODEI,<sup>14</sup> E. ORLANDO,<sup>44,45,14</sup>  
J. F. ORMES,<sup>52</sup> D. PANEQUE,<sup>53</sup> M. PERSIC,<sup>45,54</sup> M. PESCE-ROLLINS,<sup>5</sup> V. PETROSIAN,<sup>14</sup> R. PILLERA,<sup>13,6</sup> G. PRINCIPE,<sup>44,45,27</sup>  
S. RAINÒ,<sup>13,6</sup> R. RANDO,<sup>9,10,8</sup> B. RANI,<sup>34,48</sup> M. RAZZANO,<sup>4,5</sup> A. REIMER,<sup>55</sup> O. REIMER,<sup>55</sup> M. SÁNCHEZ-CONDE,<sup>56,57</sup>  
P. M. SAZ PARKINSON,<sup>58</sup> D. SERINI,<sup>6</sup> C. SGRÒ,<sup>5</sup> E. J. SISKIND,<sup>59</sup> P. SPINELLI,<sup>13,6</sup> D. TAK,<sup>60</sup> L. TIBALDO,<sup>61</sup>  
D. F. TORRES,<sup>62</sup> J. VALVERDE,<sup>48,34</sup> Z. WADIASINGH,<sup>34,47</sup> AND W. ZHANG<sup>63</sup>

<sup>1</sup>Center for Cosmology and Particle Physics Phenomenology, University of Southern Denmark, Campusvej 55, DK-5230 Odense M, Denmark

<sup>2</sup>Istituto Nazionale di Fisica Nucleare, Sezione di Perugia, I-06123 Perugia, Italy

<sup>3</sup>Department of Physics and Astronomy, Clemson University, Kinard Lab of Physics, Clemson, SC 29634-0978, USA

<sup>4</sup>Università di Pisa, Dipartimento di Fisica E. Fermi, I-56127 Pisa, Italy

<sup>5</sup>Istituto Nazionale di Fisica Nucleare, Sezione di Pisa, I-56127 Pisa, Italy

<sup>6</sup>Istituto Nazionale di Fisica Nucleare, Sezione di Bari, I-70126 Bari, Italy

<sup>7</sup>Università degli studi di Trento, via Calepina 14, 38122 Trento, Italy

<sup>8</sup>Istituto Nazionale di Fisica Nucleare, Sezione di Padova, I-35131 Padova, Italy

<sup>9</sup>Dipartimento di Fisica e Astronomia “G. Galilei”, Università di Padova, Via F. Marzolo, 8, I-35131 Padova, Italy

<sup>10</sup>Center for Space Studies and Activities “G. Colombo”, University of Padova, Via Venezia 15, I-35131 Padova, Italy

<sup>11</sup>Instituto de Astrofísica de Canarias and Universidad de La Laguna, Dpto. Astrofísica, 38200 La Laguna, Tenerife, Spain

<sup>12</sup>California State University, Los Angeles, Department of Physics and Astronomy, Los Angeles, CA 90032, USA

<sup>13</sup>Dipartimento di Fisica “M. Merlin” dell’Università e del Politecnico di Bari, via Amendola 173, I-70126 Bari, Italy

<sup>14</sup>W. W. Hansen Experimental Physics Laboratory, Kavli Institute for Particle Astrophysics and Cosmology, Department of Physics and SLAC National Accelerator Laboratory, Stanford University, Stanford, CA 94305, USA

<sup>15</sup>Istituto Nazionale di Fisica Nucleare, Sezione di Torino, I-10125 Torino, Italy

<sup>16</sup>Dipartimento di Fisica, Università degli Studi di Torino, I-10125 Torino, Italy

<sup>17</sup>Deutsches Elektronen Synchrotron DESY, D-15738 Zeuthen, Germany

<sup>18</sup>Institut für Theoretische Physik and Astrophysik, Universität Würzburg, D-97074 Würzburg, Germany

<sup>19</sup>INAF-Istituto di Astrofisica Spaziale e Fisica Cosmica Milano, via E. Bassini 15, I-20133 Milano, Italy

<sup>20</sup>Istituto Nazionale di Fisica Nucleare, Sezione di Roma “Tor Vergata”, I-00133 Roma, Italy

<sup>21</sup>Space Science Data Center - Agenzia Spaziale Italiana, Via del Politecnico, snc, I-00133, Roma, Italy

<sup>22</sup>Dipartimento di Fisica, Università La Sapienza, Piazzale A. Moro, 2, I-00185 Roma, Italy

<sup>23</sup>Dipartimento di Fisica, Università degli Studi di Perugia, I-06123 Perugia, Italy

<sup>24</sup>Italian Space Agency, Via del Politecnico snc, 00133 Roma, Italy

<sup>25</sup>Friedrich-Alexander Universität Erlangen-Nürnberg, Erlangen Centre for Astroparticle Physics, Erwin-Rommel-Str. 1, 91058 Erlangen, Germany

<sup>26</sup>Friedrich-Alexander-Universität, Erlangen-Nürnberg, Schlossplatz 4, 91054 Erlangen, Germany

<sup>27</sup>INAF Istituto di Radioastronomia, I-40129 Bologna, Italy

<sup>28</sup>Grupo de Altas Energías, Universidad Complutense de Madrid, E-28040 Madrid, Spain

<sup>29</sup>Università di Pisa and Istituto Nazionale di Fisica Nucleare, Sezione di Pisa I-56127 Pisa, Italy

<sup>30</sup>Department of Physical Sciences, Hiroshima University, Higashi-Hiroshima, Hiroshima 739-8526, Japan

<sup>31</sup>Dipartimento di Fisica, Università di Roma “Tor Vergata”, I-00133 Roma, Italy

- <sup>32</sup> *Dipartimento di Fisica e Geologia, Università degli Studi di Perugia, via Pascoli snc, I-06123 Perugia, Italy*
- <sup>33</sup> *The George Washington University, Department of Physics, 725 21st St, NW, Washington, DC 20052, USA*
- <sup>34</sup> *Astrophysics Science Division, NASA Goddard Space Flight Center, Greenbelt, MD 20771, USA*
- <sup>35</sup> *University of North Florida, Department of Physics, 1 UNF Drive, Jacksonville, FL 32224, USA*
- <sup>36</sup> *Laboratoire Leprince-Ringuet, CNRS/IN2P3, École polytechnique, Institut Polytechnique de Paris, 91120 Palaiseau, France*
- <sup>37</sup> *Yunnan Observatories, Chinese Academy of Sciences, Kunming 650216, China*
- <sup>38</sup> *Department of Physics, KTH Royal Institute of Technology, AlbaNova, SE-106 91 Stockholm, Sweden*
- <sup>39</sup> *The Oskar Klein Centre for Cosmoparticle Physics, AlbaNova, SE-106 91 Stockholm, Sweden*
- <sup>40</sup> *NASA Postdoctoral Program Fellow, USA*
- <sup>41</sup> *Department of Astronomy, University of Science and Technology of China, Hefei 230026, China*
- <sup>42</sup> *School of Astronomy and Space Science, University of Science and Technology of China, Hefei 230026, China*
- <sup>43</sup> *Institute of Astrophysics, Foundation for Research and Technology-Hellas, Heraklion, GR-70013, Greece*
- <sup>44</sup> *Dipartimento di Fisica, Università di Trieste, I-34127 Trieste, Italy*
- <sup>45</sup> *Istituto Nazionale di Fisica Nucleare, Sezione di Trieste, I-34127 Trieste, Italy*
- <sup>46</sup> *The Aerospace Corporation, 14745 Lee Rd, Chantilly, VA 20151, USA*
- <sup>47</sup> *Department of Astronomy, University of Maryland, College Park, MD 20742, USA*
- <sup>48</sup> *Center for Space Science and Technology, University of Maryland Baltimore County, 1000 Hilltop Circle, Baltimore, MD 21250, USA*
- <sup>49</sup> *Hiroshima Astrophysical Science Center, Hiroshima University, Higashi-Hiroshima, Hiroshima 739-8526, Japan*
- <sup>50</sup> *Vatican Observatory, Castel Gandolfo, V-00120, Vatican City State*
- <sup>51</sup> *Department of physics and Astronomy, Louisiana State University, Baton Rouge, LA 70803, USA*
- <sup>52</sup> *Department of Physics and Astronomy, University of Denver, Denver, CO 80208, USA*
- <sup>53</sup> *Max-Planck-Institut für Physik, D-80805 München, Germany*
- <sup>54</sup> *INAF-Astronomical Observatory of Padova, Vicolo dell'Osservatorio 5, I-35122 Padova, Italy*
- <sup>55</sup> *Institut für Astro- und Teilchenphysik, Leopold-Franzens-Universität Innsbruck, A-6020 Innsbruck, Austria*
- <sup>56</sup> *Instituto de Física Teórica UAM/CSIC, Universidad Autónoma de Madrid, E-28049 Madrid, Spain*
- <sup>57</sup> *Departamento de Física Teórica, Universidad Autónoma de Madrid, 28049 Madrid, Spain*
- <sup>58</sup> *Santa Cruz Institute for Particle Physics, Department of Physics and Department of Astronomy and Astrophysics, University of California at Santa Cruz, Santa Cruz, CA 95064, USA*
- <sup>59</sup> *NYCB Real-Time Computing Inc., Lattingtown, NY 11560-1025, USA*
- <sup>60</sup> *SNU Astronomy Research Center, Seoul National University, Seoul 08826, Republic of Korea*
- <sup>61</sup> *IRAP, Université de Toulouse, CNRS, UPS, CNES, F-31028 Toulouse, France*
- <sup>62</sup> *Institute of Space Sciences (ICE, CSIC), Campus UAB, Carrer de Magrans s/n, E-08193 Barcelona, Spain and Institut d'Estudis Espacials de Catalunya (IEEC), E-08034 Barcelona, Spain and Institució Catalana de Recerca i Estudis Avançats (ICREA), E-08010 Barcelona, Spain*
- <sup>63</sup> *Institute of Space Sciences (ICE, CSIC), Campus UAB, Carrer de Magrans s/n, E-08193 Barcelona, Spain; and Institut d'Estudis Espacials de Catalunya (IEEC), E-08034 Barcelona, Spain*

(Accepted July 11, 2025)

## ABSTRACT

The steady-state gamma-ray emission from the Sun is thought to consist of two emission components due to interactions with Galactic cosmic rays: (1) a hadronic disk component, and (2) a leptonic extended component peaking at the solar edge and extending into the heliosphere. The flux of these components is expected to vary with the 11-year solar cycle, being highest during solar minimum and lowest during solar maximum, as it varies with the cosmic-ray flux. No study has yet analyzed the flux variation of each component over solar cycles.

In this work, we measure the temporal variations of the flux of each component over 15 years of *Fermi* Large Area Telescope observations and compare them with the sunspot number and Galactic cosmic-ray flux from AMS-02 near Earth.

We find that the flux variation of the disk anticorrelates with the sunspot number and correlates with cosmic-ray protons, as expected, confirming its emission mechanism. In contrast, the extended component exhibits a more complex variation: despite an initial anticorrelation with the sunspot number, we find neither anticorrelation with the sunspot number nor correlation with cosmic-ray electrons over the full 15-year period. This most likely suggests that cosmic-ray transport and modulation in the

inner heliosphere are unexpectedly complex and may differ for electrons and protons or, alternatively, that there is an additional, unknown component of gamma rays or cosmic rays.

These findings impact space weather research and emphasize the need for close monitoring of Cycle 25 and the ongoing polarity reversal.

*Keywords:* The Sun (1322) — Gamma-Rays (637) — Cosmic Rays (329)

## 1. INTRODUCTION

Over the last fifteen years, the Sun has been observed to be a gamma-ray source in its quiet state (Orlando & Strong 2008), i.e., in its non-flaring state or non-flaring regions. Hudson (1989) and Seckel et al. (1991) made the first calculations of the gamma-ray emission from pion decay by Galactic Cosmic Ray (CR) cascades in the solar atmosphere. This emission was expected to be confined to the region of the solar disk. The flux was expected to vary during the solar cycle, as observed for the lunar gamma-ray flux (Thompson et al. 1997), which is produced by similar mechanisms. The existence of a spatially extended inverse Compton (IC) component from scattering by CR electrons on solar photons was theorized by Moskalenko et al. (2006) and Orlando & Strong (2007) independently. This broad emission was expected to be brighter at the solar edges and roughly inversely proportional to the angular distance from the Sun, as recently confirmed by refined IC models (Orlando & Strong 2021). Recent theoretical studies have also focused on improving models of the disk component (e.g., Zhou et al. 2017; Niblaeus et al. 2019; Mazziotta et al. 2020; Becker Tjus et al. 2020; Gutiérrez & Masip 2020; Hudson et al. 2020; Li et al. 2024a,b).

Due to their association with CRs, the intensity of both the disk and extended components of the gamma-ray emission from the quiet Sun is predicted to vary over the solar cycle and, in particular, to anticorrelate with the sunspot number (SSN), and to correlate with the CR flux as measured near Earth.

The first evidence of the gamma-ray emission from the quiet Sun was found by Orlando & Strong (2008) by analyzing the entire archival EGRET data. However, the limited sensitivity of EGRET precluded the investigation of flux variation over time. The launch of the *Fermi* Gamma-Ray Space Telescope in 2008 enabled observations of the quiet Sun with high statistical significance. Observations of solar emission during the first 18 months of the *Fermi* Large Area Telescope (LAT) mission, a time period during solar minimum, were reported in Abdo et al. (2011) and were in agreement with Orlando & Strong (2008). Variations of the solar flux with solar activity were first reported by Ng et al. (2016) with six years of *Fermi*-LAT observations. They found the

gamma-ray flux of the solar emission to be larger during solar minimum than during solar maximum. More recent works (Tang et al. 2018; Linden et al. 2022) updated the analysis over almost the entire 11-year cycle and found that the solar flux varies by nearly a factor of two between the solar maximum and the solar minimum. Moreover, Linden et al. (2022) found that the variation in the 0.1–10 GeV range is not dependent on energy, differing from what was expected. More recent observations with HAWC (Albert et al. 2023) showed the solar flux extending to TeV energies during solar minimum, and an upper limit during solar maximum was observed.

In summary, the observed solar gamma-ray flux variations have confirmed a trend of anticorrelation with the solar activity. However, the extended IC component has not been included in these studies. Hence, contamination of the disk flux measurement by the extended component is not excluded in previous works. To date, no studies have examined the correlation of the two distinct components with CR proton and electron fluxes, or their anticorrelation with solar activity. In this letter, we report results for 15 years of *Fermi*-LAT observations of the Sun, allowing us to distinguish the two solar components and to study their flux variations over Solar Cycle 24 and the first years of Solar Cycle 25.

## 2. METHOD

We use observations with *Fermi*-LAT (Atwood et al. 2009), which detects gamma rays from 20 MeV to over 300 GeV. In survey mode, the LAT observes the full sky approximately every 3 hours with an almost uniform daily exposure. This capability, combined with its large field of view of  $\sim 2.4$  sr (at 1 GeV) and high sensitivity, allows us to observe the Sun daily.

### 2.1. Data Selection

We analyze 15 years of *Fermi*-LAT observations, specifically from 2008 August 4 to 2023 June 30 in the 70 MeV – 70 GeV energy range. We select the Pass 8 SOURCE event class (Atwood et al. 2013; Bruel et al. 2018) and P8R3\_SOURCE\_V6 instrument response

functions<sup>64</sup>, and excluded times when the LAT was within the South Atlantic anomaly. To reduce contamination from cosmic-ray interactions with the upper atmosphere, events with zenith angles larger than  $90^\circ$  are excluded. Because the Sun is moving across the sky, the analysis of its emission requires special handling. In addition to the standard *Fermi*-LAT Science Tools package<sup>65</sup>, dedicated tools are used where data are selected in a moving frame centered on the instantaneous position of the Sun, which is computed using an interface to the JPL ephemeris libraries<sup>66</sup>. As in *Abdo et al. (2011)*, to further reduce contamination while maintaining useful data, we apply a carefully customized selection: data are excluded when the Sun is within  $30^\circ$  of the Galactic plane,  $20^\circ$  of the Moon, and  $10^\circ$  of the four bright sources along its path (3C 454.3, PSR J1620–4927, Geminga, and the Crab Nebula). In addition, all solar flares listed in the LAT Solar Flare Catalog (*Ajello et al. 2021*) are removed. Also, to remove any contamination from fainter solar flares and other flaring or bright sources close to the path of the Sun, in this work we develop a dedicated procedure involving the monitoring of light curves in nested regions centered on the Sun. After inspection, we remove the time intervals when short variations of light curve fluxes exceed  $5\sigma$  from the average flux value, using 3-hour time bins. These cuts produce a very clean event sample by removing about 55% data in total.

## 2.2. Background Evaluation

After applying our data cuts, there may still be possible contamination in the region around the Sun from diffuse Galactic and isotropic gamma-ray emissions, as well as from weak point sources along the ecliptic. This contamination is referred to as background. Correct evaluation of the background is essential for analyzing solar emission, as IC emission extends beyond  $20^\circ$  from the Sun (*Orlando & Strong 2007*).

As in *Abdo et al. (2011)*, we determine the background by applying the off-source (or “fake” source) method: an imaginary source follows the path of the Sun along the ecliptic but at a different time, which means at a different distance from the real Sun. The data sample we use for the background determination is centered on the off-source position and has the same selection cuts applied to the data sample of the Sun. For a careful

evaluation of the background, we compute seven fake sources from  $90^\circ$  to  $270^\circ$  from the Sun in steps of  $30^\circ$ . Moreover, we divide the 15-year dataset into 2-year sub-samples, each starting six months after the previous one, on which we perform the binned maximum likelihood technique as described by *Mattox et al. (1996)*, using *gtlike* as included in the *Fermitools*. We do it by iteratively adjusting the energy spectrum in order to maximize the likelihood of the data given the model. We find the seven background fluxes to be within  $\pm 3\%$  of their average values. Following *Abdo et al. (2011)*, this 3% variation defines the systematic uncertainty on the solar components. Then, we use the output of the likelihood analysis for each time interval as the background model for the corresponding data set centered on the Sun.

## 2.3. Analysis of the Solar Components

We evaluate the gamma-ray flux variation over time by dividing the 15-year dataset into 2-year sub-samples, each each starting six months after the previous one, similar to the procedure for the background. For the binned maximum likelihood analysis we use a bin size of  $0.1^\circ$  and the energy dispersion (*edisp\_bins*=−2). Three components are considered simultaneously in the analysis: the solar disk component, the solar extended component, and the background. The latter is fixed as previously described and masked over the solar disk. We model the disk with emission confined within a radius of  $0.265^\circ$  from the solar center, corresponding to the average radius of the Sun. We model the extended component with emission starting from the edge of the solar disk and decreasing inversely with the elongation angle from the Sun, following solar IC emission models (*Orlando & Strong 2007, 2008, 2021*), as in *Abdo et al. (2011)*. Both energy spectra are modeled with a log-parabolic function. The solar model components are convolved with the energy-dependent point-spread function, while the background component is not, because it is derived from observational data.

## 3. TEMPORAL VARIATION RESULTS

The two components are clearly separately measured<sup>67</sup> and their flux variations are integrated over 2-year sub-samples. Then, the disk and extended component variations are compared with the flux of CR protons (*Aguilar et al. 2021*) and CR electrons (*Aguilar et al. 2023*), respectively, and with the SSN<sup>68</sup>.

<sup>64</sup> P8R3 data do not contain the residual background events near the Ecliptic present in P8R2, which could have affected the analysis

<sup>65</sup> *Fermitools* version 2.2.0,  
<https://fermi.gsfc.nasa.gov/ssc/data/analysis/software/>

<sup>66</sup> <https://ssd.jpl.nasa.gov/horizons/>

<sup>67</sup> The significance of the detection of each component is verified for each data point, being the  $TS > 300$ .

<sup>68</sup> SSN data are downloaded from the World Data Center SILSO, [https://www.sidc.be/SILSO/DATA/SN\\_ms\\_tot\\_V2.0.txt](https://www.sidc.be/SILSO/DATA/SN_ms_tot_V2.0.txt)

The correlation between these datasets (solar flux, CR flux, SSN) is visually inspected and statistically investigated by calculating the Pearson correlation coefficient (Pearson 1920, 1931, 1932) and the z-transformed discrete correlation function (zDCF)<sup>69</sup> (Alexander 2013; Edelson & Krolik 1988; Blandford & McKee 1982). The eventual time lag between datasets is also evaluated. For a proper correlation study, the datasets of *Fermi*-LAT, the daily CR fluxes, and the monthly SSN are interpolated or averaged over the same time bin of 30 days. We test the robustness of the results using non-overlapping 2-year sub-samples, each starting six months after the previous one, to verify that the results are not sensitive to the choice of sub-sample start times. Since solar flux variations in sub-samples are integrated over 2-year periods starting every six months, an apparent trend on a timescale shorter than 2 years should not be interpreted as physically meaningful.

The results for the two components are reported below.

### 3.1. Disk Component

Figure 1 shows details of the disk emission. Panel (a) shows the flux variation expressed as a fraction of the average flux of the disk component for energies greater than 250 MeV, 500 MeV, and 1 GeV over time. The regions with different shades of gray represent the systematic uncertainties. The variations in the three integral energy ranges are synchronous and the variation of the disk flux with the solar cycle is clearly demonstrated. For all three energy ranges, the disk flux varies by  $\pm 40\%$  with respect to the average value. Panel (b) shows the anticorrelation between the disk flux variation above 1 GeV and the SSN over time. This is consistent with expectations, as CR-induced emission is expected to vary over the solar cycle in anticorrelation with solar activity (e.g., Thompson et al. 1997; Ng et al. 2016). Panel (c) shows correlation between the disk flux variation above 1 GeV and the temporal variation of the CR proton flux at  $\sim 2$  GeV as observed by AMS-02. Hence, the hadronic emission of the disk component around GeV energies is correctly identified. This also means that the modulation of CR protons at Earth is temporally coincident with the modulation at the Sun within the 2-year resolution of the gamma-ray fluxes. Panel (d) shows correlation between the solar disk flux above 1 GeV and the lunar flux (Ackermann et al. 2016). The

lunar flux variations throughout the period (Loparco et al. 2024) show a similar trend. This corroborates the theory that both solar disk and lunar emission share a similar production mechanism. The comparisons in Panels (b), (c), (d) give Pearson and zDCF correlations (or anti-correlations) above 0.9<sup>70</sup> with no significant time lag.

### 3.2. Spatially Extended Component

Figure 2 shows details of the extended component. Panel (a) shows the flux variation expressed as a fraction of the average flux of the solar extended component for energies greater than 250 MeV, 500 MeV, and 1 GeV over time. The gray-shaded regions represent its systematic uncertainties. For the three integral energy ranges, the flux varies by  $+40\%$  and  $-60\%$  between its maximum and minimum values. In comparison to the disk emission, the systematic errors for the extended component are larger due to the uncertainties in the background estimation.

The extended flux variation above 1 GeV is compared with the sunspot number (panel (b) of the same figure) and with the temporal variation of the CR electron<sup>71</sup> flux at 1 GeV as observed by AMS-02 (panel (c)). The plots show a complex relationship between the extended component flux variation and both the SSN and CR electron flux. Indeed, the correlation coefficients over the entire period are below 0.3, indicating no significant correlation. Because the periods before 2011 lack CR electron measurements from AMS-02, to gain insights on this complex trend of the extended component, panel (d) shows a temporal comparison between the flux variations of the extended component and the disk. A visual comparison of panels (b), (c), and (d) appears to reveal periods consistent with expectations, as well as periods contrary to them. The correlation coefficients with the disk flux variation and the sunspot number, calculated only for the period from August 2008 to July 2012, show strong correlation and anti-correlation (above 0.9), respectively, in line with expectations.

## 4. DISCUSSION AND CONCLUSIONS

We report for the first time the temporal variation of the flux of both distinct gamma-ray components of the solar emission over 15 years of *Fermi*-LAT observations. In the following, we discuss the two solar emission components separately.

<sup>69</sup> Because the Pearson coefficient may not be accurate for non-linear relationships (Yule 1926; Scargle 2020; Riechers & Crutchfield 2021) we also use zDCF, which is better suited for temporal cross-correlations and commonly applied to non-linear cases.

<sup>70</sup> We find this value for the non-overlapping 2-year sub-samples, and also for all data points.

<sup>71</sup> The IC component also includes positrons, but their flux accounts for at most a few percent of the total.



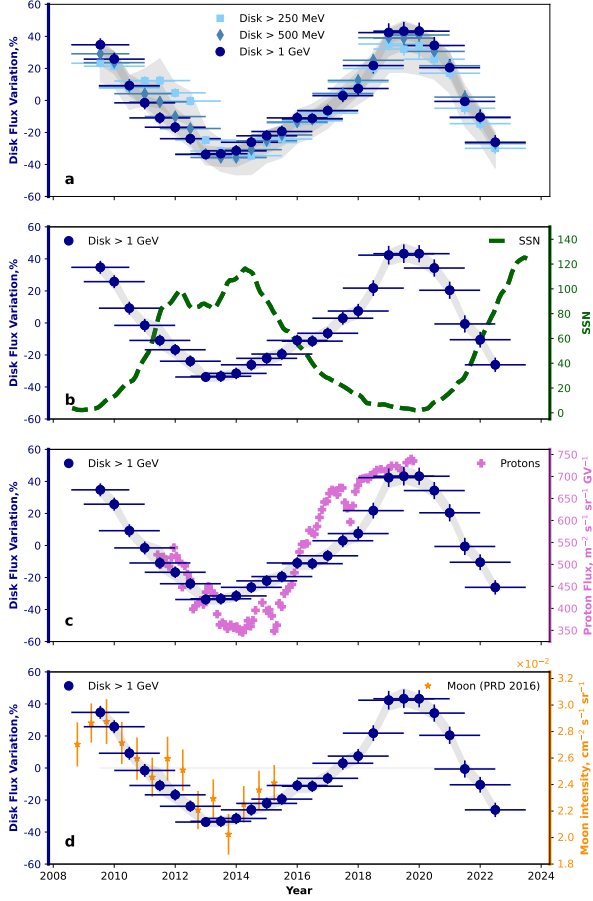


**Figure 1.** Panel (a): Percentage of the flux variation of the solar disk component above 25 MeV, 500 MeV, and 1 GeV versus time in year. For normalization, the average flux values used are  $9.15$ ,  $4.69$ ,  $2.23$  ( $\times 10^{-8} \text{ cm}^{-2} \text{ s}^{-1}$ ), respectively. The gray regions define systematic uncertainties. Panel (b): flux variation in time of the solar disk component above 1 GeV compared with the SSN. Panel (c): flux variation in time of the solar disk component above 1 GeV compared with the CR proton flux at 2.14–2.4 GV (Aguilar et al. 2021). Panel (d): flux variation in time of the solar disk component above 1 GeV compared with the Moon’s flux above 56 MeV (Ackermann et al. 2016).

The flux variation in time of the disk anticorrelates with the sunspot number and correlates with cosmic-ray protons, confirming its emission mechanism. It generally agrees with the results of Linden et al. (2022) obtained for a shorter period. Possible differences are attributable to different temporal binning and data selections. Interestingly, we find that the variation in time is independent of energy above 250 MeV, whereas the flux in the lowest energy range is expected to vary the

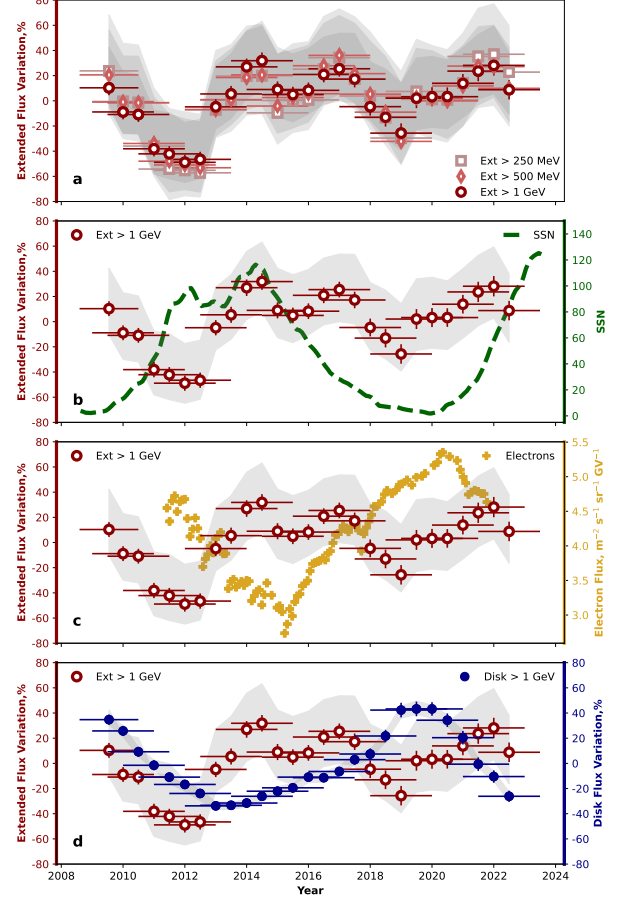


**Figure 2.** Panel (a): Percentage of the flux variation of the solar extended component above 250 MeV, 500 MeV, and 1 GeV versus time. For normalization, the average flux values used are  $30.00$ ,  $13.99$ ,  $5.95$  ( $\times 10^{-8} \text{ cm}^{-2} \text{ s}^{-1}$ ), respectively. The gray region defines systematic uncertainties. Panel (b): flux variation of the solar extended component above 1 GeV compared with the SSN. Panel (c): flux variation of the solar extended component above 1 GeV compared with the CR electron flux at 1.00–1.71 GV (Aguilar et al. 2023). Panel (d): flux variation of the solar extended component above 1 GeV compared with the flux variation of the disk component above 1 GeV.

most<sup>72</sup> due to the stronger modulation of CRs at lower energies. The fact that the relative variation of fluxes does not depend on energy was already anticipated by Linden et al. (2022). It can be an indication that the solar magnetic field plays an important role in the variability, as the intricate structure of the field at the Sun would lead to complex energy and time variations.

<sup>72</sup> Calculations in Mazziotta et al. (2020) around solar maximum might suggest weak energy independence, though this remains speculative due to limited coverage and the absence of calculations during solar minimum.

The variation of the extended component has not been investigated before<sup>73</sup>. We find temporal anticorrelation between the extended flux variation and the SSN from 2008 August to 2012 June, and correlation between the extended flux variation and the disk variation over the same period. However, for 2013–2023, we no longer observe any correlation/anticorrelation, not even with the CR electron flux. Similarly to the disk, the variation is independent of energy.

The variations of the extended component come as a surprise and challenge current theoretical models and assumptions. We do not provide a definitive interpretation of these results; instead, we highlight related observational and modeling challenges to illustrate the complexity of the topic. For example, in the outer heliosphere, it has long been accepted that CR electrons are modulated similarly to protons (e.g., [Gleeson & Axford 1968](#)) and that their modulation anticorrelates with the SSN. However, several studies on heliospheric CR propagation beyond 1 AU have reported indications, based on measurements (e.g., [Aguilar et al. 2018](#)) and models (e.g., [Potgieter 2013](#); [Potgieter & Vos 2017](#); [Tomassetti et al. 2017, 2022](#); [Caballero-Lopez et al. 2019](#)), that CR modulation and propagation depend on the particle’s charge sign and the solar magnetic polarity. For protons, [Tomassetti et al. \(2017\)](#) proposed a simple predictive model of solar modulation in the outer heliosphere that depends on the SSN and the tilt angle to explain the observed time lag between solar activity data and CR measurements. This time lag is found to depend on the solar polarity. Recently, in order to explain the modulation over time of the AMS-02 CR electrons, [Aslam et al. \(2023\)](#) calculated that particle drift in the outer heliosphere becomes negligible during the period when the polarity is not well defined and starts recovering just after the polarity reversal, but the mean free path keeps decreasing or remains unchanged for some period after the polarity reversal. On the other hand, the propagation of CR electrons, in the inner heliosphere, i.e., within 1 AU of the Sun, has received comparatively little attention. A recent study on cosmic-ray transport in the inner heliosphere ([Petrosian et al. 2023](#)) shows that electrons undergo multiple scattering due to turbulence and experience significant energy losses as they approach the Sun. Based on this, we expect that at higher energies the reduced electron flux near the Sun under stronger magnetic fields would decrease the IC emission, reinforcing the expected anticorrelation with solar activity.

While most of the current literature focuses on CR propagation in the outer heliosphere rather than in the inner heliosphere, our present results suggest that the details of CR electron transport and modulation in the inner heliosphere are even more complex than in the outer heliosphere. Hence, models of CR electron propagation that work beyond 1 AU may not be extrapolated down to the Sun. Modulation and propagation within 1 AU of the Sun have rarely been studied because of poor observational constraints. Our work can shed light on the propagation of CRs in the inner Galaxy through the study of the variation of the CR-induced emission from the Sun.

Curiously, at the end of 2012, the reversal of the Sun’s polar magnetic field began, which resulted in the change of polarity in Cycle 24. In contemporary with the reversal, unexplained asymmetric emission from the Sun in the GeV range has recently been observed ([Arsioli & Orlando 2024](#)). Interestingly, the polarity reversal was unusual ([Janardhan et al. 2018](#); [Upton & Hathaway 2023](#)) with the south polarity flipping in 2013, while the north polarity being delayed to the end of 2014.

Our results also suggest, as do other studies (e.g. [Tang et al. 2018](#); [Linden et al. 2018](#)), a possible crucial role of the solar magnetic field, which remains unexplained. Possibly, CR electron transport and modulation models in the inner heliosphere may be constrained by observations of synchrotron radiation in X-rays produced by these electrons interacting with the solar magnetic field, as recently theorized by [Orlando et al. \(2023\)](#). Other effects may also play an important role (e.g., [Puzzoni et al. 2024](#); [Ng et al. 2024](#); [Mazziotta 2025](#)).

Our results may even call into question whether the spatially extended emission is produced mainly by Galactic CR electrons. This may potentially include an unknown additional mechanism of gamma-ray production or an additional component of high-energy CR close to the Sun. Both hypotheses would need to be investigated further.

To conclude, the discovery reported in this work presents an additional challenge to our understanding of the Sun in gamma rays. This adds to the detection of the solar unexplained spectral dip ([Linden et al. 2018](#)), the observations of an unexpected asymmetry in GeV emission from the disk ([Arsioli & Orlando 2024](#)), and the detection of GeV and TeV solar emission at higher energies than expected ([Abdo et al. 2011](#); [Linden et al. 2018](#); [Albert et al. 2023](#)). A revision of current models and timely observations of CRs and the Sun during the current Cycle 25, as well as during the reversal in polarity, all will help in understanding the unexpected

<sup>73</sup> After completing this work and the manuscript, we became aware of a related study by [Linden et al. \(2025\)](#), which had just appeared on arXiv.

trend of the solar extended emission and its relation to the solar cycles.

## 5. ACKNOWLEDGMENTS

The *Fermi*-LAT Collaboration acknowledges generous ongoing support from a number of agencies and institutes that have supported both the development and the operation of the LAT as well as scientific data analysis. These include the National Aeronautics and Space Administration and the Department of Energy in the United States, the Commissariat à l’Energie Atomique and the Centre National de la Recherche Scientifique / Institut National de Physique Nucléaire et de

Physique des Particules in France, the Agenzia Spaziale Italiana and the Istituto Nazionale di Fisica Nucleare in Italy, the Ministry of Education, Culture, Sports, Science and Technology (MEXT), High Energy Accelerator Research Organization (KEK) and Japan Aerospace Exploration Agency (JAXA) in Japan, and the K. A. Wallenberg Foundation, the Swedish Research Council and the Swedish National Space Board in Sweden. Additional support for science analysis during the operations phase is gratefully acknowledged from the Istituto Nazionale di Astrofisica in Italy and the Centre National d’Études Spatiales in France. This work was performed in part under DOE Contract DE-AC02-76SF00515. Partial support from NASA grant No. 80NSSC20K1558 and 80NSSC22K0495 is acknowledged.

## REFERENCES

- Abdo, A. A., Ackermann, M., Ajello, M., et al. 2011, *ApJ*, 734, 116
- Ackermann, M., Ajello, M., Albert, A., et al. 2016, *PhRvD*, 93, 082001
- Aguilar, M., Cavasonza, L. A., Ambrosi, G., et al. 2021, *PhRvL*, 127, 271102
- Aguilar, M., Cavasonza, L. A., Ambrosi, G., et al. 2023, *PhRvL*, 130, 161001
- Albert et al. 2023, *PhRvL*, 131, Issue 5, 051201
- Alexander, T. 2013, *arXiv:1302.1508*
- Atwood, W. B. et al. 2009, *ApJ*, 697, 1071
- Atwood, W., Albert, A., Baldini, L., et al. 2013, *arXiv:1303.3514*
- Aguilar, M., Cavasonza, L. A., Ambrosi, G., et al. 2018, *PhRvL*, 121, 051102
- Arsioli, B. & Orlando, E. 2024, *ApJ*, 962, 52
- Ajello, M. et al. 2021, *ApJS*, 252, 13
- Aslam, O. P. M., Luo, X., Potgieter, M. S., et al. 2023, *ApJ*, 947, 72
- Becker Tjus, J., Desiati, P., Döpper, N., et al. 2020, *A&A*, 633, A83
- Blandford, R. D. , McKee, C. F., 1982, *ApJ*, 255, 419B
- Bruel, P. et al. 2018, *arXiv:1810.11394*
- Caballero-Lopez, R. A., Engelbrecht, N. E., & Richardson, J. D. 2019, *ApJ*, 883, 73
- Edelson, R. A. , Krolik, J. H., 1988, *ApJ*, 333, 646E2
- Gleeson, L. J. & Axford, W. I. 1968, *ApJ*, 154, 1011
- Gutiérrez, M. & Masip, M. 2020, *Astroparticle Physics*, 119, 102440
- Hudson, H. S. 1989, *Proc Gamma Ray Observatory Workshop (Greenbelt: Goddard Space Flight Center)*, 4-351
- Hudson, H. S., MacKinnon, A., Szydlarski, M., et al. 2020, *MNRAS*, 491, 4852
- Janardhan, P., Fujiki, K., Ingale, M., et al. 2018, *A&A*, 618, A148
- Li, J.-T., Beacom, J. F., Griffith, S., et al. 2024, *ApJ*, 961, 167
- Li, Z., Ng, K. C. Y., Chen, S., et al. 2024, *Chinese Physics C*, 48, 045101
- Linden, T., Zhou, B., Beacom, J. F., et al. 2018, *PhRvL*, 121, 131103
- Linden, T., Beacom, J. F., Peter, A. H. G., et al. 2022, *PhRvD*, 105, 063013
- Linden, T., Li, J.-T., Zhou, B., et al. 2025, *arXiv:2505.04625*
- Loparco et al. 2024, 11th International Fermi Symposium, College Park, Maryland, USA
- Mattox, J. R., et al. 1996, *ApJ*, 461, 396
- Mazziotta, M. N., Luque, P. D. L. T., Di Venere, L., et al. 2020, *PhRvD*, 101, 083011
- Mazziotta, M. N. 2025, *arXiv:2505.18275*
- Moskalenko, I. V., Porter, T. A., & Digel, S. W. 2006, *ApJL*, 652, L65
- Ng, K. C. Y., Beacom, J. F., Peter, A. H. G., et al. 2016, *PhRvD*, 94, 023004
- Ng, K. C. Y., Hillier, A., & Ando, S. 2024, *arXiv:2405.17549*
- Niblaeus, C., Beniwal, A., & Edsjö, J. 2019, *JCAP*, 2019, 011
- Orlando, E., Petrosian, V., & Strong, A. 2023, *ApJ*, 943, 173
- Orlando, E. & Strong, A. W. 2007, *Ap&SS*, 309, 359
- Orlando, E., & Strong, A. W. 2008, *A&A*, 480, 847
- Orlando, E. & Strong, A. 2021, *JCAP*, 04, 004



- Pearson, K.F.R.S. 1920, *Biometrika*, Volume 13, Issue 1, October 1920, Pages 25–45
- Pearson, Egon S. *Journal of the American Statistical Association*, 1931, Volume 26, Pages 128-134
- Pearson, Egon S. 1932, *Journal of the American Statistical Association*, Volume 27, Pages 424-426
- Petrosian, V., Orlando, E., & Strong, A. 2023, *ApJ*, 943, 1, 21
- Potgieter, M. S. 2013, *Living Reviews in Solar Physics*, 10, 3
- Potgieter, M. S. & Vos, E. E. 2017, *A&A*, 601, A23
- Puzzoni, E., Fraschetti, F., Kóta, J., et al. 2024, *ApJ*, 973, 2, 118
- Riechers, P. M. & Crutchfield, J. P. 2021, *Physical Review Research*, 3, 013170
- Scargle, J. D. 2020, *ApJ*, 895, 90
- Seckel, D., Stanev, T., & Gaisser, T. K. 1991, *ApJ*, 382, 652
- Tang, Q.-W., Ng, K. C. Y., Linden, T., et al. 2018, *PhRvD*, 98, 063019
- Thompson, D. J., Bertsch, D. L., Morris, D. J., & Mukherjee, R. 1997, *J. Geophys. Res.*, 102, 14735
- Tomassetti, N., Orcinha, M., Barão, F., et al. 2017, *ApJL*, 849, L32
- Tomassetti, N., Bertucci, B., & Fiandrini, E. 2022, *PhRvD*, 106, 103022
- Upton, L. A. & Hathaway, D. H. 2023, *Journal of Geophysical Research (Space Physics)*, 128, e2023JA031681
- Yeo, K. L., Krivova, N. A., Solanki, S. K., et al. 2023, *A&A*, 679, A25
- Yule, G. Udny, 1926, *Journal of the Royal Statistical Society*, 19, 1–63
- Zhou, B., Ng, K. C. Y., Beacom, J. F., et al. 2017, *PhRvD*, 96, 023015